The Impact of Compressive Misfit Strain on Improper Ferroelectricity in Lead Titanate/Strontium Titanate Superlattices

By Juliana Coraor

Abstract:

Because of their unique properties, ferroelectric materials are used in electronic devices as piezoelectrics in actuators and in electric field sensors, and as dielectrics in capacitors. Their electrical characteristics are strictly controlled by their crystalline structure, and as such, modifications to the latter influence the former. Structural changes in ferroelectric materials can be achieved through the growth of superlattices, that is, alternating layers of two materials, or by the application of strain. These changes in structure can induce new characteristics such as improper ferroelectricity, which is manifested in the superlattices through an increase in tetragonality as thickness decreases, and produces a high dielectric constant with little temperature dependency. If strain can be used to further increase the improper ferroelectricity of these superlattices, these superlattices could have farther reaching applications in electronic devices because they would be resistant to heating during use.

The purpose of this study was to investigate the effect of compressive epitaxial strain on the improper ferroelectricity found in lead titanate/strontium titanate (PTO/STO) superlattices at high percentages of STO. PTO/STO superlattices 50 nm thick were grown on LSAT substrates, which have lattice parameters smaller than those of STO, in order to apply compressive strain. Samples with varying numbers of PTO layers for every three STO layers were analyzed using high resolution four-circle x-ray diffraction in order to determine their average out-of-plane lattice parameters. These values were used to compute the tetragonality of each superlattice which was then compared with the tetragonality values of non-strained PTO/STO superlattices. It was confirmed that the structures of lead titanate and strontium titanate could be modified though growth on substrates with different lattice parameters to produce both compressive and tensile strain, and that these strain-induced modifications were able to be sustained up to a film thickness of approximately 60 nm. Using these results, it was found through the tetragonality that the improper ferroelectricity exhibited by these superlattices was greatly diminished by the application of compressive misfit strain. These conclusions suggest that if tensile strain was applied, improper ferroelectricity could be increased, and these superlattices would become more resistant to the effects of temperature. As capacitors are accompanied by high electrical discharge that produces unwanted heat loss due to resistance, a temperature resistant dielectric material would dramatically increase their efficiency.

I. Introduction

Ferroelectrics have electrical properties that make them desirable for a variety of technological and industrial applications. Recent work has been done on constructing ferroelectric nano-devices, such as nanocapacitors[1] and nanoshell tubes[2]. Both have potential as components in memory devices[1]; nanoshell tubes may further be used in microfluidic device systems. Since ferroelectrics also possess characteristics such as piezoelectric and amplified dielectric properties that arise from symmetry conditions for ferroelectricity, they can be used in transistors and in piezoelectric sensors and actuators. Research has been ongoing to understand how to modify ferroelectrics to maximize their desired qualities and minimize the ones that are detrimental to specific applications. This requires understanding of the effects of changes in crystal structure on ferroelectric behavior. This work specifically investigates the effects of structural changes induced by misfit (epitaxial) strain on ferroelectricity in superlattice thin films.

A. Ferroelectrics

When an external electric field applied to a material distorts the cloud of electrons around nuclei in a net direction opposite to the electric field, it is said to show electric polarization. Ferroelectrics are materials that can maintain an electric polarization without needing a continuous applied electric field (Fig. 1). The electric polarization of these materials can be switched by applying an opposite external electric field. All ferroelectrics have additional properties that exist because of symmetry requirements of the ferroelectric properties. They must all be piezoelectric, which means that they produce an electric field when compressed, or undergo a change in size when exposed to an electric field. They also must be pyroelectric, that is, they produce an electric field when undergoing a change in temperature, and dielectric, which simply means that the

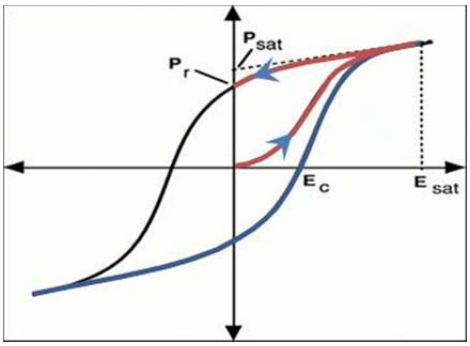

Figure 1. Classic electric polarization hysteresis loop of a ferroelectric material. Initially when there is zero net polarization (arrowed curve at the origin) an electric field (E_C) can be applied to create a positive polarization in the material (arrowed curve). This reaches the saturation polarization (P_{sat}) at the field saturation (E_{sat}). When the external electric field is reduced to zero, the polarization remains but decreases to the value of the remnant polarization (P_r). An opposite field can be applied to reverse the polarization of the material.[3]

material becomes electrically polarized when an external electric field is applied (ferroelectricity implies that it must be a reversible, spontaneous polarization). Because ferroelectrics have symmetry constraints, their atomic structure must be ordered, that is, they must have a crystalline structure.

B. Crystal structure

A crystalline material is composed of repeating atom arrangements. The smallest repeating unit that contains all of the symmetry elements is referred to as a unit cell. Every crystalline solid must belong to one of a set of fourteen possible structural arrangements called the Bravais lattices.[4] The Bravais lattices fall into 7 crystal classes: triclinic, monoclinic, rhombohedral, hexagonal, orthorhombic, tetragonal, and cubic. Each lattice is described by specific symmetry elements, lattice dimensions (parameters), and angles between the principal axes (Fig. 2).[4] The lattices of greatest importance to this study are in the cubic, tetragonal, and orthorhombic classes. In a cubic lattice, the three angles (α, β, and γ) between the *a*, *b*, and *c* axes are equal to 90°. Furthermore, each of its lattice parameters (*a*, *b*, and *c*) are equal. Tetragonal lattices are similar to cubic ones in that all of the angles between the principle axes are 90° degrees; however, only two of the three axes (*a* and *b*) are of equal length. This makes 2 of three unique faces rectangular and one square. It can be considered a distortion from a cube by stretching or compressing a cube along one of the three axes. Orthorhombic structures have no sides equal to one another and distortion from a cube must involve two axes.

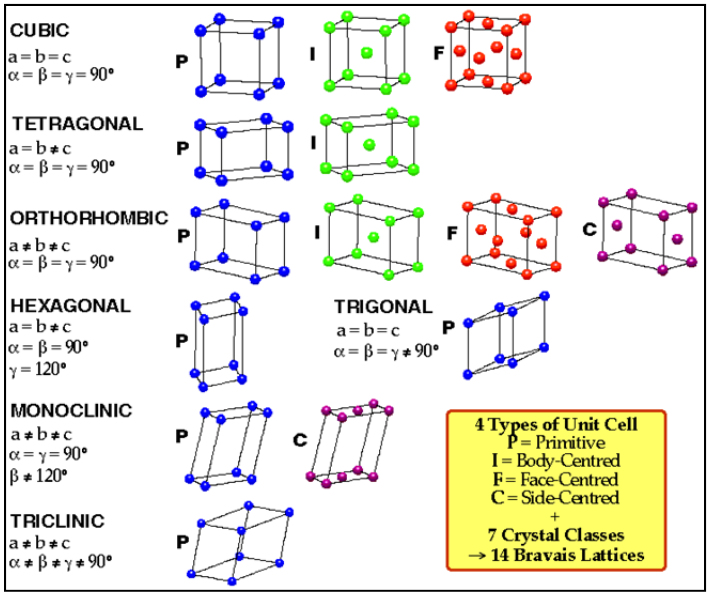

Figure 2. These are the fourteen Bravais lattices that compose all of the possible atomic arrangements of crystals. The figure labeled trigonal in this diagram is simply a rhombohedral structure.[20]

Each crystal lattice can be primitive, face centered, base centered, and body centered. These terms refer to the existence of atoms (of the same element as those in the corners) in the unit cell in places besides at the eight corners. Primitive means that there are none of those ions in places other than the

corners. Face centered describes a crystal that has ions at each corner of the cell as well as in the center of each face of the crystal. Base centered is similar, but it only has ions in two opposing faces, not in all six of them. Body centered crystal lattices have an ion in the center of the crystal as well as in the corners. All of these classifications are critical in determining the specific chemical and electrical properties of minerals, as the special arrangements of each of the ions in a crystal have drastic effects on the interactions between them and their environment.

Perovskites are a group of crystalline materials with structures similar to that of calcium titanate (which is the actual mineral perovskite). Most deviate slightly from a cubic structure with slight symmetry reducing distortions caused by over- or undersized cations. Their chemical formula is usually $A^{2+}B^{4+}X_3^{2-}$, with A in twelve-fold coordination, and B in eight-fold coordination with X. When the ions are too small or too large relative to the ideal cubic structure, they often rotate or shift off-center to compensate.

Lead titanate (PTO) is an oxide perovskite with the chemical formula $PbTiO_3$. It is tetragonal when at a temperature below 760 K, and cubic above 760 K at ambient pressure.[5] In the tetragonal state, its in-plane lattice parameters (if oriented in a thin film such that the square cross-section is parallel to the substrate surface) *a* and *b* are each equal to 3.905 Å; its out-of-plane lattice parameter *c* (i.e., the lattice parameter perpendicular to the surface) is equal to 4.152 Å.[9] The tetragonal structure is an important characteristic in inducing ferroelectric properties. The oxygen octahedron that encloses each titanium ion (Fig. 3) can undergo a non-centrosymmetric shift, which creates an electric polarization because of the charge on the octahedra (a net charge of -8). Tetragonal crystals can only have out-of-plane polarization, or polarization perpendicular to the surface, because the octahedra can only move along the *c* axis. This specific polarization is linked to the tetragonality, or the *c/a* ratio of the lattice

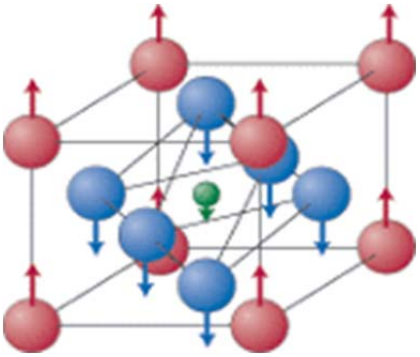

Figure 3. - A perovskite lattice centered around the small B atom (titanium ion in the center) which shows the origin of lead titanate's ferroelectric polarization. It is due to shifting of the oxygen octahedra with respect to the lead ions (which are located at the corners). [6]

parameters, of the material. As the tetragonality increases, the displacement of the octahedra from the center of the unit cell can increase.

Additional perovskites of importance to this work are shown in Table 1.

Material	Chemical Formula	Structure	Lattice Parameters	Pseudocubic lattice parameter	Ferroelectric properties
Strontium Titanate (STO)	$SrTiO_3$	Cubic	a = 3.905 Å	n/a	Incipient Ferroelectric
LSAT	$(La,Sr)(Al,Ta)O_3$	Cubic	a = 3.87 Å	n/a	Paraelectric
Dysprosium Scandate	$DyScO_3$	Orthorhombic	a = 5.44 Å b = 5.71 Å c = 7.89 Å	(a = 3.94 Å)	Paraelectric

Table 1 - Perovskite oxides considered in this study and their respective lattice parameters, structures, and ferroelectric properties.[7] Paraelectricity is equivalent to "non"-ferroelectricity, and incipient ferroelectricity is at the border between ferroelectricity and paraelectricity.[8]

C. Improper Ferroelectricity

Ferroelectric materials are often grown in thin films for electronic applications. Different techniques have been used to modify thin-films of ferroelectric material in order to enhance desired properties. One technique involves growing alternating layers of two different materials on a substrate to create a "superlattice". The properties of superlattices often differ from those of either single material, as the combination of the two materials creates an entirely different structure.

PTO/STO superlattices are structures that are made from alternating lead titanate (ferroelectric, tetragonal) and strontium titanate (paraelectric, cubic) layers. When the abundance of lead titanate is decreased by reducing the thickness of its layer in each repetition, the superlattice exhibits behavior that deviates from that expected. One would anticipate that when the amount of ferroelectric material (the tetragonal PTO) in a PTO/STO superlattice is decreased, the superlattice structure would become less tetragonal and more cubic and therefore, ferroelectricity of the whole would decrease as well. However, instead of diminishing the extent of tetragonality, the tetragonality actually increases to some extent before decreasing to the null tetragonality of pure strontium titanate. This results from a new feature

known as "improper" ferroelectricity. In improper ferroelectricity, the oxygen octahedra rotate within the crystals and couple with the regular non-centrosymmetric shifting of the ions to enhance the polarization.[9]

Improper ferroelectricity in PTO/STO superlattices has been found to be accompanied by an abnormally high dielectric constant with no temperature dependency.[10] Usually, these two characteristics are not found together, but these superlattices display both. Possibly by altering these superlattices, these characteristics might be able to be refined in the future to allow ferroelectric superlattices to have additional applications as strong dielectrics. Before this can be done, however, we need to be able understand more about how improper ferroelectricity arises and determine a variety of ways to alter these superlattices and investigate the effect of the alteration on improper ferroelectricity.

D. Epitaxial/Misfit Strain

One method of altering the structure of these superlattices is by applying strain.[16] When a material is deposited on a substrate, atoms in the thin film (composed of one material) or superlattice (composed of two materials) attempt to align with the atoms of the substrate. If the materials in the film and the substrate have different in-plane lattice parameters, strain arises in the film as it attempts to conform to the substrate. This strain is referred to as *misfit* or *epitaxial* strain. The cumulative misfit strain will increase as the films are grown thicker; however, this increase is limited. Eventually the film will relax, and the structure will revert back to that of the pure substance.

If the film material is composed of a tetragonal substance such as lead titanate, the crystals may become more or less tetragonal (that is, more or less cubic) as compressive or tensile strain is applied. Lead titanate has an *a* lattice parameter similar to that of strontium titanate, so negligible strain develops in it when it is grown on STO. Substrates with smaller lattice parameters such as LSAT should apply in-plane compressive strain to PTO, whereas substrates with larger lattice parameters such as $DyScO_3$ should apply in-plane tensile strain.

Although it is recognized that misfit strain can affect the tetragonality and hence, polarization, of single composition materials such as lead titanate,[15] less is known about its affect on superlattices. ***This study investigates the potential for misfit strain to affect the tetragonality of PTO/STO superlattices,***

and, through the link between tetragonality and improper ferroelectricity, to affect the extent of improper ferroelectricity.

II. Experimental Design

The effect of compressive misfit strain on tetragonality (and improper ferroelectricity) was studied by first growing thin films of PTO on LSAT, STO, and $DyScO_3$ substrates to confirm that the substrates were capable of inducing the intended type of strain. Next, a series of lead titanate thin films of different thicknesses were deposited on LSAT to determine the thickness at which they relax, and therefore how thick the superlattices could be made. Finally, superlattices with different ratios of PTO layers to STO layers were grown on LSAT and their tetragonalities quantified using x-ray diffraction. These data were used to provide evidence for the likely effect of compressive strain on improper ferroelectricity.

III. Materials & Methods

A. Growing Films

All films were grown on a substrate of the desired material with substrate dimensions of approximately 0.5 cm x 0.5 cm x 0.5 mm thick. The surface of each substrate was cleaned before the thin film or superlattice was grown on it in order to prevent contamination that could lead to strain modification. Cleaning was done ultrasonically, first in an ethanol bath and then an acetone bath. Afterwards, the substrate was removed and the surface dried with a nitrogen blower to remove any remnant particles that would contaminate the surface. The substrate was affixed to a heater using silver paste (silver paste is a good heat conductor). The heater was placed in an oven for one hour to allow the paste to harden, after which it was taken out and allowed to cool.

The superlattices and thin film materials were sputtered onto the substrate. This process involves several sputtering guns that operate inside a vacuum chamber (Fig. 4). At the proper vacuum pressure inside the chamber, ionized argon and oxygen molecules are released into the chamber. They bombard a

target attached to the sputtering gun made of whichever material is meant to be deposited, and cause target molecules to be ejected from the solid target. This process is assisted by plasma in the sputtering gun contained by electric and magnetic fields that gives energy to the target molecules. The target molecules collect on the substrate attached to the heater that is hung upside down in the chamber. By varying which targets are exposed by raising and lowering the shutters in front, one can vary the number of layers of the target material that is deposited onto the substrate. Different target materials can be attached to each gun to allow multiple materials to be deposited in alternation.

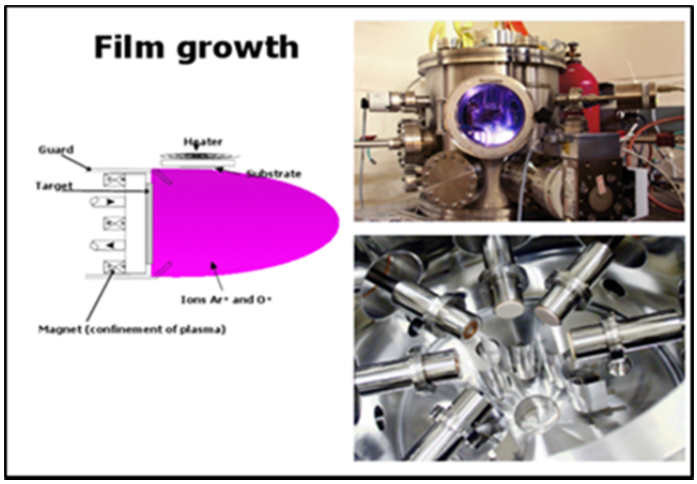

Figure 4. The diagram on left illustrates the different components of the sputter gun. The top right shows the vacuum chamber. The bottom right demonstrates the different sputter guns, each with targets composed of different materials.

Before the superlattice experiments were conducted, several characteristics of the effect of misfit strain on the deposited materials had to be investigated. First, it had to be confirmed that misfit strain could indeed be applied to the material of interest and that it would change the tetragonality of that material. Second, the thickness to which the material could be grown before it relaxed had to be evaluated. For example, if this maximum thickness was only 10 or 20 nm, clearly growing a standard superlattice of 50 nm or greater in thickness would not be possible.

Three different substrate materials, LSAT, $DyScO_3$, and $SrTiO_3$ were used to confirm that strain can be successfully applied to a film material. This evaluation was conducted on thin films of lead titanate instead of on a superlattice, because the tetragonality of thin films is much easier to determine than that of superlattices. The films were deposited at a temperature of 550°C, an argon flow of 12 SCCM, an oxygen flow of 7 SCCM, and a pressure inside the vacuum chamber of 0.18 mbar. The firing rates were determined by the observed growth rates of each material, for PTO it was 2.72 minutes/layer, for STO it was 2.1 minutes/layer. 20 nm films were deposited on each substrate, and the tetragonality of each was determined using a high resolution 4-circle x-ray diffractometer (Bruker D8). In addition, a series of lead

titanate thin films were grown on LSAT at different thicknesses in order to evaluate the maximum thickness at which it can be grown before the PTO relaxes. These were also analyzed using the x-ray diffractometer.

Finally, PTO-STO superlattices were grown on LSAT substrates. The ratio of PTO to STO layers was varied in order to vary the composition of the superlattice and also the number of interfaces. As end markers on the compositional variance, 20 nm pure PTO and pure STO thin films were grown on LSAT as well. The number of layers of STO in each superlattice was kept at 3 unit cells; superlattices with PTO/STO ratios of 12:3, 6:3, 3:3, 2:3, and 1:3 were grown under the same conditions as the thin films mentioned above. Once a thin film or superlattice was grown in the sputtering chamber, the chamber was vented with nitrogen and the heater with the film attached was removed. The film was scraped off of the heater and the silver paste using a scalpel, and then placed in a sample container and brought to the x-ray diffractometer for analysis in order determine their average *c* lattice parameter.

B. Structural Analysis.

The structural analysis of the thin films was done using thin film x-ray diffraction. X-ray diffraction works on the principles of constructive interference of rays diffracted by the different planes of a crystal. The wavelength of an x-ray is approximately equal to the radius of a single atom, so x-rays can pass between the atoms of a crystal or be diffracted by atoms in a specific layer. After these parallel x-rays penetrate the crystal, those that are diffracted by atoms in different unit cell layers exit out of phase with respect to each other. They destructively interfere, thereby cancelling each other out at all θ angles (i.e., the angle between the incident beam and the plane of the crystal) except at the specific angles that fulfill the Bragg equation: $2d\sin\theta = m\lambda$, (where d is the out-of-plane lattice parameter, m is reflection order, and λ is the wavelength of the x-rays).[11] The reflection order refers to the number of whole wavelengths by which each diffracted ray exiting the crystal differs. The phase difference between two beams that were diffracted by two different layers could be any multiple of 2π if they constructively interfere, so m is just equal to the phase difference divided by 2π. (Fig. 5)

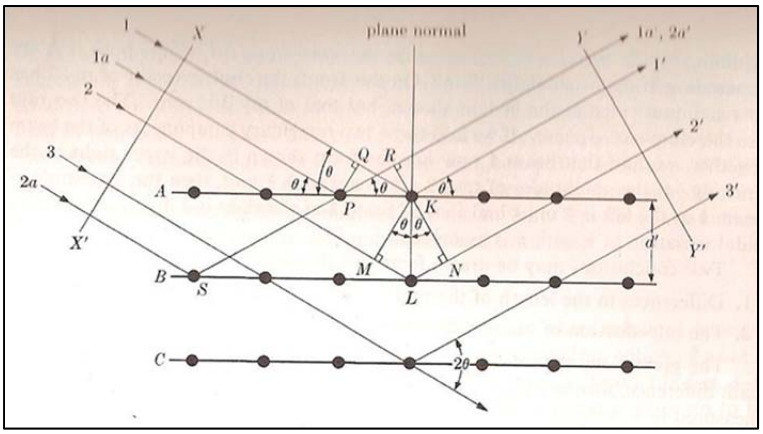

Figure 5. The diagram to the left demonstrates the origin of Bragg's law in terms of the interference from x-rays diffracting off of different planes in a crystal. A crystalline structure with atomic layers A, B, and C with a separation of length d is subjected to x-rays coming it at an angle θ with respect to the layers of atoms. The length that ray 2 takes through the crystal (equal to 2dsinθ through trigonometric constraints) must be equal to a whole number of wavelengths or else it will not constructively interfere with ray 1 and form a diffraction peak. If it does constructively interfere, the value of θ at which this occurs is referred to as the Bragg angle of the material.[12]

This principle is often used to determine the out-of-plane lattice parameter of a crystal because all the other values in this equation are known. The wavelength of the x-rays in an x-ray diffractometer is usually equal to the $K\alpha_1$ wavelength, 1.545 Å,[12] which is the strongest x-ray emission released by a copper atom when it moves from the excited state to the ground state. The reflection order starts at zero at $\theta = 0°$ and increases at each diffraction peak by one as θ increases. For example, the first peak at $\theta > 0°$ has an m of one, the second an m of two, etc.[12] In a multiple circle x-ray diffractometer the 2θ angle (the angle between the detector and the x-ray source) is varied by moving the sample and the detector with respect to the x-ray source until a diffraction maximum is recorded. At that maximum the Bragg law is achieved, and that angle can be used to determine the *c* lattice parameter (value of d in the Bragg equation) of the material. [Again the greater the c/a lattice parameters vary from 1, the greater the tetragonality.]

To analyze the samples, each thin film was placed onto a glass slide that sits on top of a set of motors that allow the sample to be rotated in numerous directions in between the x-ray source and the detector. A scan of the x-ray intensity over an interval of 2θ (angle between the detector and the x-ray source) and Ω (angle between the sample and the x-ray source), also referred to as a 2θ/Ω scan, was performed. The θ angle of the film or superlattice in each sample was found by examining the highest peak of each (disregarding the substrate peak) and dividing the 2θ value by two. Because the angle of incidence is equal to the angle of reflection, the θ value gained through this process should be equal to the

θ in the Bragg equation. This was inserted into the Bragg equation to determine the *c* lattice parameter of each of the thin films and superlattices.

IV. Data Analysis

A. Compressive and Tensile Strain

The three 20 nm lead titanate thin films grown on dysprosium scandate, LSAT, and STO were examined using thin film x-ray diffraction. Because of their respective lattice parameters, $DyScO_3$ was expected to induce in-plane tensile strain and cause the *c* lattice parameter of the lead titanate to decrease while LSAT was expected to induce compressive strain and cause the *c* lattice parameter to increase.

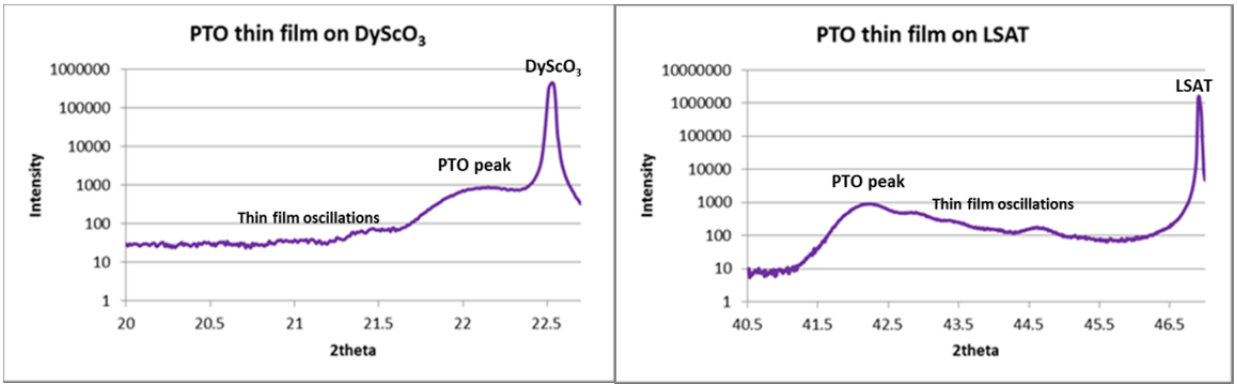

Figure 6. To the left is a $2\theta/\Omega$ scan of the 001 substrate peak (i.e.- first order reflection) and 001 film peaks of lead titanate on $DyScO_3$. The respective peaks and oscillations are labeled. The right graph is of the 002 peaks, or second order reflections, of the PTO thin film on LSAT.

The results from $2\theta/\Omega$ scans of the strained samples can be seen in Figure 6. The narrow peaks in each graph are from the substrates; the broad shoulders are from the thin films. In a perfect crystal with an infinite number of layers, the diffracted x-rays leaving the crystal destructively interfere except at the exact angle of Bragg's law, giving rise to a peak with a width of close to zero. However, when the number of layers is limited as in a thin film, not all of the x-rays are cancelled out. This produces a broader peak and secondary oscillations, as seen in the graphs (Fig. 6). The difference in interval between the film peaks and the substrate peaks in the two graphs indicates that dysprosium scandate induces a different effect on PTO thin films than LSAT.

Compared to the 4.1520 Å of bulk lead titanate, the resulting *c* value of the lead titanate thin film on $DyScO_3$ was equal to 4.0200 Å; on LSAT it was 4.2650 Å; on $SrTiO_3$ it was equal to 4.1375 Å. Incorporating these values into the formula for mechanical out-of-plane strain, $e = \frac{\Delta l}{l}$ where Δl is the change in out-of-plane lattice parameter and l is the original c value, e($DyScO_3$) = -0.0318, e(LSAT) = 0.0272, and e(STO) = -0.0035. These values for each of the different substrates quantitatively demonstrated that $DyScO_3$ applies in-plane tensile strain (out-of-plane compressive strain, though the convention is to refer to in-plane strain), LSAT induces in-plane compressive strain, and $SrTiO_3$ imposes negligible strain.

B. Relaxation Thickness

LSAT was picked as the substrate for the relaxation thickness experiments because of all of the non-STO substrates, it was the only one with a cubic structure, and therefore its lattice parameters were the easiest to quantify. The dysprosium scandate substrates did not exhibit the same lattice parameters on our x-ray diffractometer as recorded in the literature, so these were not used.

A series of lead titanate films were grown on LSAT substrates at different thicknesses. The thicknesses and the calculated PTO out-of-plane lattice parameters can be seen in Figure 7.

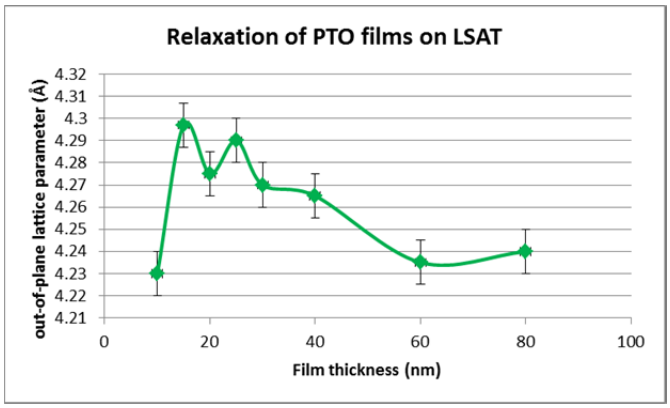

Figure 7. Graph of the out-of plane lattice parameter (*c*) of each sample versus sample thickness. The film relaxes at a thickness of approximately 60 nm (where, *c* reaches a minimum). The low value of *c* for the 10 nm sample could be due to depolarization effects that occur when the sample is a few unit cells thick.[15]

Figure 7 shows that between 40 and 60 nm thickness, a strong decrease in out-of-plane lattice parameters occurs as the thickness of the lead titanate increases. This is indicative of the start of relaxation, as the strain applied by the LSAT on the PTO at the epitaxial interface begins to be become

less significant compared to the lowest energy stable configuration of the bulk lead titanate, and the extent of tetragonality starts to lessen. Relaxation appears to occur at a thickness of approximately 60 nm.

There is a noticeably lower *c* value for the 10 nm thick sample than for the 15-40 nm samples (Fig. 7). This is most likely caused by the greater influence of depolarization fields at thicknesses on the order of a few unit cells. If the electric field of a ferroelectric film is not cancelled at the boundaries of the film, its field would extend beyond the film, which creates a high energy state. What can happen is the development of multiple domains of opposite polarization in the film that cancel each other to reduce the overall field.[13] Field reduction can also occur through screening by free electrons in electrodes attached to each side of the film.[13] When screening occurs, electrons build up at the interfaces between the electrodes and the film and counteract the film's electric field (created by the bound charges in the unit cells). However, perfect screening is hard to create, as the compensating electrons are not exactly at the boundary and therefore do not cause the overall electric field to drop to zero immediately at the interface.[14] This leads to an imperfect cancellation of charge which creates net charges at the boundaries between each electrode and the film that induce another electric field to occur opposite to the film polarization. This is known as a depolarization field, and acts against the film polarization. At thicknesses of several unit cells, the effect of the depolarization field becomes substantial and causes the polarization and tetragonality to decrease.[15]

Standard three-dimensional representations of a crystal use the three axes *h*, *k*, and *l*, where *h* and *k* are in-plane and *l* is out-of-plane. 2θ/Ω scans (e.g., Fig. 7) can only give information about the out-of-plane axis *l* (that is, in the c crystallographic direction). Reciprocal space maps, on the other hand, are useful for examining the in-plane lattice parameters. Reciprocal space represents each plane (or side) of a crystal as a vector normal to the surface. The distances between two atoms within the crystal are equal to the reciprocals of the lengths of the vector. A reciprocal space map (RSM) is produced by a series of measurements taken by the x-ray diffractometer in reciprocal space in two crystal dimensions, in this case *h* and *l*.

RSMs were made of the 40 nm and the 80 nm thick PTO/STO thin films in order to examine the extent of relaxation at these specific thicknesses in more detail. (Figure 8) The lead titanate thin films were observed to have at least partially relaxed in-plane at a thickness of 80 nm. This is indicated by the asymmetrical region on the right map in Figure 8 where the in-plane lattice parameters (*h* and *k*) have begun to change as the lead titanate reverts back to its original size and shape. The out-of-plane parameter (*l)* has also decreased, which would occur with the start of relaxation.

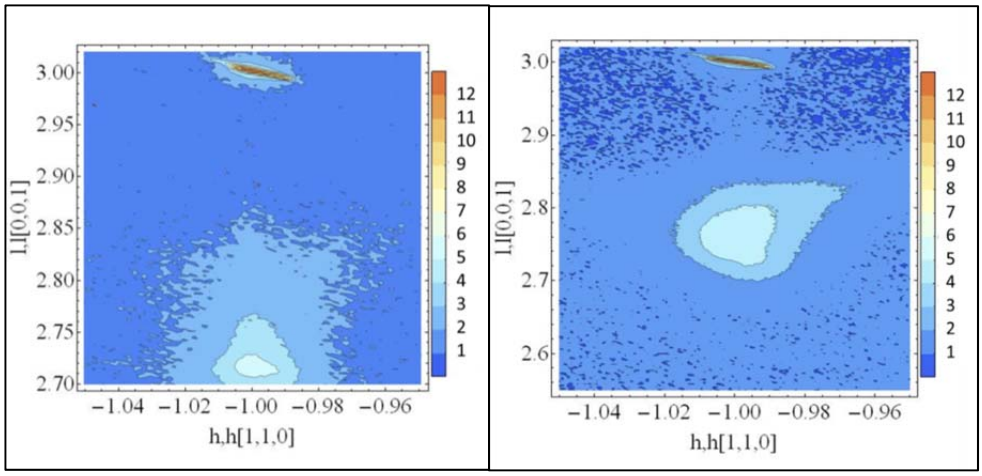

Note to Evaluator from SSP- You may request a color copy of this page from SSP Staff.

Figure 8. The two images seen above are reciprocal space maps around the 113 (*hkl)* superlattice peak. The color represents x-ray intensity and can be interpreted using the color scale to the right of each map. The left image is of the 40 nm film. The narrow diagonal strip near the top is from the substrate, and the larger, less intense spot at the bottom of the map originates from the film. The image to the right is of the 80 nm sample. It shows evidence of relaxation, as indicated by the elongation of the film peak in the *h* direction.

C. PTO/STO Superlattices and Improper Ferroelectricity

In order to relate the effect of superlattice structure on improper ferroelectricity, it is important that the structure of the superlattice be well known. A 2θ/Ω scan was performed on each of the superlattices to look for what are known as superlattice diffraction peaks. The 2θ versus intensity graphs of a superlattice are significantly different from those of a thin film because of the superlattice's multiple periodicities. A 2θ/Ω scan on an x-ray diffractometer is used to measure the out-of-plane distance between unit cell repetitions, and is therefore affected by the periodicity of the layers. There are two periodicities in superlattices, one caused by the repetition of each individual layer, and one caused by the repetition of the overall superlattice pattern. Since the x-ray diffractometer operates in reciprocal space,

the smaller periodicity of the superlattice is translated into more frequent and sharper peaks, whereas the larger periodicity formed by the individual layers creates a broader and less frequent peak that is similar to what is formed by a thin film. They undergo interference with one another to form superlattice peaks with varying intensity.

Figure 9 is of a 3:3 PTO/STO superlattice. Because the superlattice periodicity is six times smaller than the individual layer periodicity (six unit cells pass before the pattern repeats), the frequency of the superlattice peaks should be six times greater than the substrate peaks. Hence, for every substrate reflection (001, 002), there are six superlattice peaks. However, the farther away from the individual layer peak, the smaller the constructive interference, which is why it is hard to see the 4th and 5th superlattice peaks (with this diffractometer).

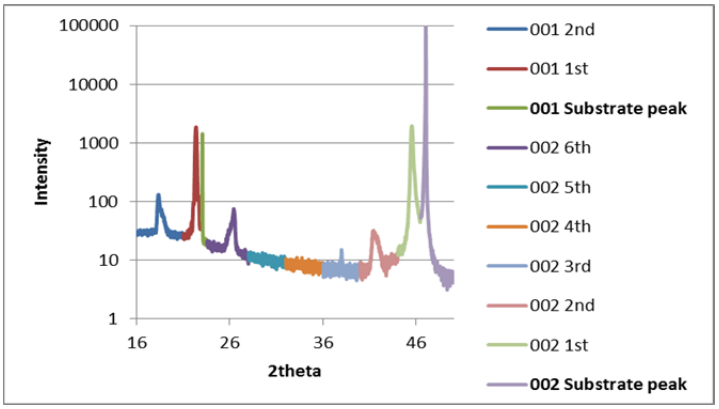

Figure 9. X-ray intensity versus 2θ angle for a 3:3 superlattice (three layers of PTO followed by 3 layers of STO). Six superlattice peaks can be seen to accompany each substrate reflection because of the difference in periodicities.

Note to Evaluator from SSP- You may request a color copy of this page from SSP Staff.

The distance between the first and second superlattice peaks for each superlattice was used to determine the superlattice periodicity of each and therefore, the number of layers that compose each repetition. Because the growth rates of each material changed as the amount of target diminished, the actual number of layers that compose each repetition were not always equal to what was desired. Table 2 illustrates the number of layers of each repetition in each superlattice as determined by the x-ray diffractometer. Because the values were close to what was expected, it was assumed that each superlattice grown had the desired number of layers.

Superlattice	Expected number of layers	Actual number of layers
1:3PTO/STO	4	3.8
2:3 PTO/STO	5	4.9
3:3 PTO/STO	6	5.6
6:3 PTO/STO	9	8.6
12:3 PTO/STO	15	14.5

Table 2 - Expected and measured number of layers of each superlattice repetition. The description of the superlattice includes the desired number of layers of each PTO and STO. The total number of layers should be equal to the sum of the number of layers of each material. Because the measured value deviates from the desired value by less than 1 layer, it can be assumed that each superlattice has the desired number of layers.

The x-ray diffractometer was also used to determine the average unit cell *c*-lattice parameter of the superlattices, as well as the tetragonality (*c/a*). The *c/a* value was found through Bragg's law, where $^{c}/_{a} = \frac{\lambda}{2\sin\theta_c} \times \frac{2\sin\theta_a}{\lambda}$. Therefore, $^{c}/_{a} = \frac{\sin\theta_a}{\sin\theta_c}$.

Without constructive interference from the individual layers, the superlattice peaks would all be at the same intensity. However, because of the broad peak created by the average unit cell lattice parameter, the superlattice peak that lies at the maximum of the broad peak will have the highest intensity value. The 2θ value at this highest peak was used to describe the average lattice parameter, which was then used to determine the tetragonality of the superlattice.

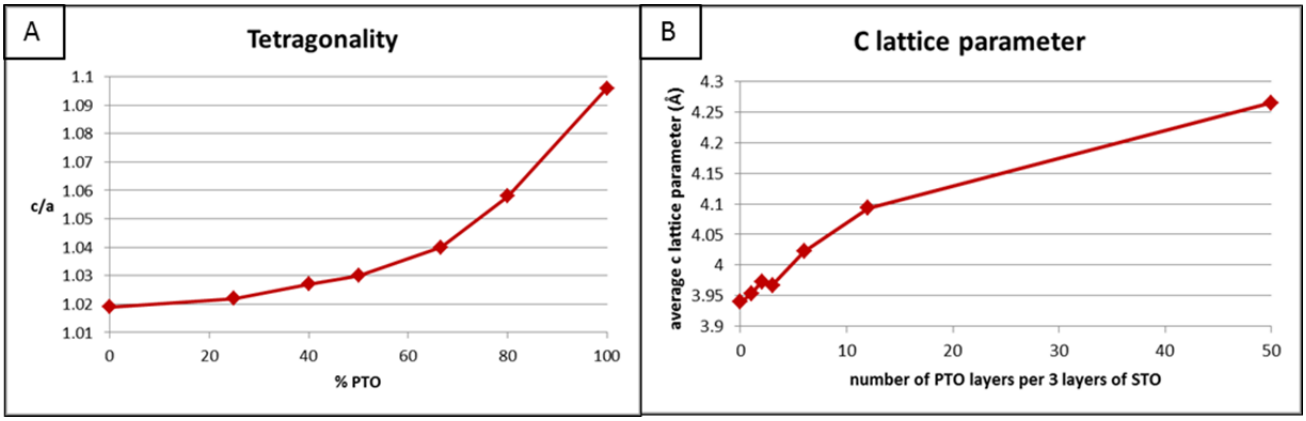

Figure 10. a.) The *c/a* ratios of the lattice parameters versus the % PTO of the whole superlattice for PTO/STO superlattices grown on a LSAT substrate. The endpoints of the graph (0% and 100%) are not of superlattices but rather of 20 nm thin films of pure STO on LSAT and pure PTO on LSAT. There is no rise in tetragonality associated with improper ferroelectricity as would be noted by a peak near 0% PTO. **b.)** Average out-of-plane lattice parameter of each superlattice versus the number of layers of PTO for every three layers of STO. (Note that the highest point on the graph at 50 layers is the 20 nm PTO film and therefore contains no layers of STO.) A slight increase in c lattice parameter can be seen near the 0% PTO endpoint.

The tetragonalities and *c*-lattice parameters of the various superlattices investigated can be seen in

Figure 10. Improper ferroelectricity would be indicated by an increase in tetragonality near the 0% endpoint on both graphs as the number of interfaces in the superlattice increases, thereby allowing more octahedral rotations. However, no noticeable increase can be seen in the tetragonality graph. A slight rise can be seen in the graph depicting the out-of-plane lattice parameters of the superlattices at the 2:3 data point, but at none of the others.

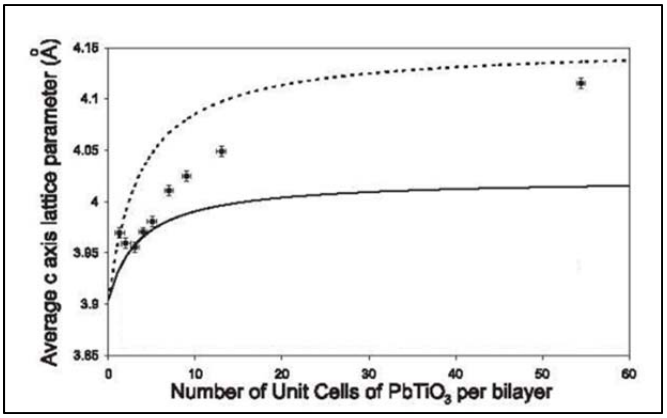

Figure 11. *c* lattice parameters of different PTO/STO superlattices grown on strontium titanate, from Dawber et al. (2005).[9] The data points are experimental values and the two lines (dashed and solid) indicate theoretical values based on paraelectric and ferroelectric states. The increasing values near the STO-rich side of the graph are much more marked than the values seen in the misfit strain experiment described here.

This observation differs from the data of Dawber et al. (2005) in which PTO/STO superlattices *without applied misfit strain* (grown on strontium titanate) were observed to have multiple superlattice *c* values that contributed to higher than normal lattice parameters governed by improper ferroelectricity[9] (Fig. 11).

V. Summary of Results

In this study it was shown that the use of substrates with varied lattice parameters was an effective technique for applying misfit strain. As can be seen in the tetragonality graph of Figure 10, the tetragonality of the pure strontium titanate thin film is approximately 1.02 ± .005, significantly different from the value of 1.0 that arises when STO is grown on an STO substrate. Furthermore, unstrained lead titanate has a tetragonality of 1.07 ± .005, lower than the strained value recorded as 1.09 ± .005. These results are consistent with theoretical studies conducted by Zembilgotov et al. (2002) which indicated that the out-of plane electric polarization of lead titanate thin films increased with compressive misfit strain[16], which would be manifested in an increase in tetragonality.

Relaxation experiments also confirmed that compressive strain applied by LSAT could be maintained up to a thickness of approximately 60 nm before relaxing. The tetragonality of the PTO thin films grown on LSAT began to decrease at 60 nm, indicating that the highly strained state of the thin film was no longer favorable at that thickness. This result is critical for determining if misfit strain is a useful tool for ferroelectric thin film and superlattice modification, and allowed experiments on 50 nm thick superlattices to be conducted.

The investigation into the improper ferroelectricity of PTO/STO superlattices under compressive misfit strain yielded the result that compressive strain acts to reduce the effect of antiferroelectric distortions (rotations of the octahedra). The rise in the average out-of-plane lattice parameter of the superlattices near the STO-rich side in Figure 10b does indicate that the improper ferroelectricity still has an influence on the tetragonality of the superlattice even in this highly strained state, but its influence is less substantial.

VI.- Implications

Misfit strain can be used to alter the properties of thin film and superlattice ferroelectrics by changing the lattice parameters of these materials. By understanding these effects, scientists in the future can use strain to develop innovative ferroelectric materials for a wide range of applications in ferroelectric memory and photocatalytic processes, as well as applications as strong piezoelectrics, dielectrics, and pyroelectrics.

It has been found in numerous studies that amplified piezoelectric responses occur at morphotropic phase boundaries, or narrow boundaries between phase fields that indicate a rapid phase change over a small interval of temperature, pressure, composition, or strain (Fig. 12).[17] These phase changes are accompanied by polarization rotations as the electric polarization of the ferroelectric material shifts from out-of-plane in a tetragonal crystal to an angle between in-plane and out-of-plane in a rhombohedral crystal.[19] Presumably by varying the strain applied to these superlattices, it might be possible to induce a morphotropic phase boundary to form which will dramatically increase the

piezoelectricity of the material at that point in the phase field. This has numerous industrial applications, as piezoelectric materials are used in both actuators that convert mechanical energy into electrical energy through compression, and in electric field sensors that change shape when exposed to an electric field.

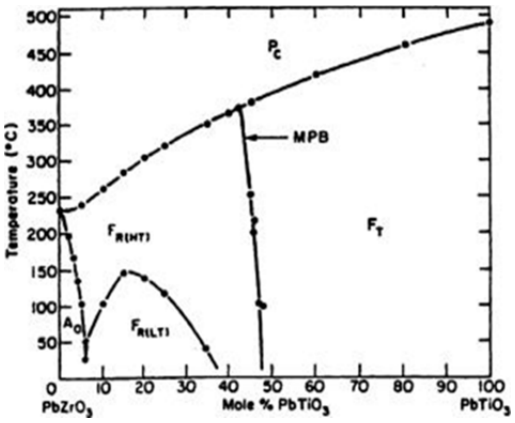

Figure 12 - A temperature versus composition phase diagram of PZT (lead zirconate/titanate solid solution), which is the leading piezoelectric used in industrial applications. The MPB is the nearly straight line between the tetragonal and rhombohedral phase fields at 52% $PbTiO_3$.[18]

Possibly the most critical application of this study involves the specific properties of improper ferroelectricity that cause these superlattices to have abnormally high dielectric constants with little temperature dependency, as this has relevance in the application of ferroelectrics as dielectrics. These substances have various uses in transistors, dielectric resonators, and most notably, capacitors.

Dielectric materials act to decrease the internal electric field within a material created by the external field of a set of charged electrodes on opposite sides of the dielectrics that are the components of a capacitor. Since $E = \rho/\varepsilon$, where E is the magnitude of the electric field between the parallel capacitor plates, ρ the charge on one plate (Q) over the area of the plate (A), and ε the relative permeability of the specific material to electric fields, a higher value of ε indicates a more effective dielectric because the dielectric reduces the internal electric field to a greater extent. The relative permeability of each material can be written in terms of the permeability of a vacuum, ε_0 and the material's dielectric constant, k, so that $\varepsilon = k\varepsilon_0$. The capacitance can be described by both of the following equations, $C = {}^{Q}/_{V}$ and $C = k\frac{\varepsilon_0 A}{d}$ where C is the capacitance, Q the charge on the electrode plates, V the voltage applied across the plates, k the dielectric constant, ε_0 the permeability of a vacuum, A the area of one plate, d the distance between the plates. Thus, when the dielectric constant is much larger than one, the capacitance

and ultimately the charge on the electrodes increase substantially, creating a capacitor with enhanced electrical properties.

Capacitors have numerous applications themselves. Certain electrical motors use starting capacitors to supply an initial potential that produce a lead in the current of a secondary circuit.[23] When placed at an angle with respect to the primary rotor, the circuit can induce a current within the primary wiring around the rotor, creating a temporary torque that is sufficient to initiate the rotation of the rotor. Once the motor reaches full speed, the starting capacitor is no longer needed and a centrifugal switch disconnects it from the secondary circuit. This specific type of capacitor is often found in air conditioner compressors, spa pumps, and heat furnaces.

Capacitors are not only susceptible to temperature changes because of the devices in which they are used (air conditioners, heat furnaces, etc…), but also because they are used to store large quantities of energy and to create significant potential differences. When they discharge, the current produced is substantial. This leads to high volumes of heat lost from resistance in the wires, and guarantees a rise in temperature. It has been shown that the dielectric constants of most materials are dependent upon temperature.[21] Specifically, for compounds with high dielectric constants at 0°C (i.e.- above 20), such as the perovskite compounds that were dealt with in this study (for which $\varepsilon \approx 600$)[10], an increase in temperature acts to decrease the value of the dielectric constant.[22] The function of each of the capacitors contained in modern technological applications is therefore compromised as the equipment increases in temperature, because the dielectric constants of the dielectrics within the capacitors decrease and cease to be as effective in increasing the capacitance.

Improper ferroelectricity provides an alternative to this reoccurring problem among dielectric materials. Because of their temperature independence, PTO/STO superlattices can retain their abnormally high dielectric constants at high temperatures and could act as acceptable replacements for these less temperature resistant dielectrics. However, the improper ferroelectricity discovered in PTO/STO superlattices could be modified, as demonstrated in this study, in order to decrease these properties using compressive strain, or hopefully to increase them using tensile strain. By enhancing the effects of

improper ferroelectricity in these superlattices, more energy efficient capacitors could be manufactured in the future using these materials in place of the common dielectrics, revolutionizing all capacitor applications including noise reducers, filters, and tuners in cell phones[21]; energy storage that prevents memory loss during power outages[23]; and pulsed power sources used in pulsed lasers, radar, fusion research, and particle accelerators.

VII. Future Work

Further work could be conducted on these compressively strained PTO/STO superlattices to gain a better understanding of the system. Electrical measurements can be taken to measure the electric polarization of each of the superlattices and confirm the existence of diminished improper ferroelectricity. Capacitance measurements can also be performed to assess the dielectric constant of each superlattice.

The next step would be to use a substrate with smaller lattice parameters to impose a larger amount of compressive strain on the superlattices. This could be used to determine if the improper ferroelectricity does eventually disappear with sufficient compressive strain. The opposite will be to grow the PTO/STO superlattices on substrates with larger lattice parameters in order to apply tensile strain. This will hopefully increase the improper ferroelectricity of the superlattices and could lead to new applications resulting from the properties that accompany such ferroelectricity. Another future set of experiments would involve growing other types of superlattices on LSAT such as PTO/$SrRuO_3$ (lead titanate/strontium ruthanate) superlattices, which have unique insulating properties, or PTO/$CaTiO_3$ (lead titanate/calcium titanate) superlattices, which have interesting piezoelectric characteristics, to determine whether the properties of these superlattices can be modified by strain as well.

References

[1] W. Lee, H. Han, A. Lotnyk, M. A. Schubert, S. Senz, M. Alexe, D. Hesse, S. Baik, U. Gösele. *Nature Nanotechnology*. **3**, 402-407 (2008).

[2] Y. Luo, I. Szafraniak, N. D. Zakharov, V. Nagarajan, M. Steinhart, R. B. Wehrspohn, J. H. Wendorff, R. Ramesh, M. Alexe. *Applied Physics Letters.* **83**, 3 (2003).

[3]D. L. Polla, L. F. Francis. *Annual Review of Materials Science*. **28**, 563-597 (1998).

[4] L.G. Berry, B. Mason. *Mineralogy*. (1959)

[5] M. Ahart, M. Somayazulu, R. E. Cohen, P. Ganesh, P. Dera, H. Mao, R. J. Hemley, Y. Ren, P. Liermann, Z. Wu. *Nature*. **451**, 545-548 (2008).

[6] Muralt, P. *Nature Materials*. **6**, 8-9 (2007).

[7] A. Posadas, M. Lippmaa, F. J. Walker, M. Dawber, C. H. Ahn, J. Triscone. "Growth and Novel Applications of Epitaxial Oxide Thin Films."

[8] E. Bousquet, P. Ghosez. "First-principles study of ferroelectric and antiferrodistortive instabilities in perovskite oxide superlattices".

[9] M. Dawber, C. Lichtensteiger, M. Cantoni, M. Veithen, P. Ghosez, K. Johnston, K. M. Rabe, J.-M. Triscone. *Physical Review Letters.* **95**, 177601 (2005)

[10] E. Bousquet, M. Dawber, N. Stucki, C. Lichtensteiger, P. Hermet, S. Gariglio, J.-M. Triscone, P. Ghosez. Nature. **452**, 732-736 (2008)

[11] S. A. Holgate, *Understanding Solid State Physics.* (2010)

[12] B. D. Cully. *Elements of X-ray Diffraction.* (1978)

[13] Y. Watanabe. *Ferroelectrics.* **401**, 61-64 (2010)

[14] D. J. Kim, J. Y. Jo, Y. S. Kim, Y. J. Chang, J. S. Lee, J-G. Yoon, T. K. Song, T. W. Noh. *Physical Review Letters.* **95**, 237602 (2005)

[15] P. Wurfel, I. P. Batra. *Physical Review B*. **8**, 5126–5133 (1973)

[16] A. G. Zembilgotov, N. A. Pertsev, H. Kohlstedt, R. Waser. *Journal of Applied Physics.* **91**, 2247 (2002)

[17] R. Guo, L. E. Cross, S-E. Park, B. Noheda, D. E. Cox, G. Shirane. *Physical Review Letters.* **84**, 23 (2000)

[18] B. Noheda, D. E. Cox, G. Shirane, J. A. Gonzalo, L. E. Cross, S-E. Park. *Applied Physics Letters.* **74**, 14 (1999)

[19] H. Fu, R. E. Cohen. *Nature.* **403** (2000)

[20] S. J. Heyes. "Structures of Simple Inorganic Solids." *Fundamental Aspects of Solids & Sphere Packing.* 1996-2000. Oxford.
<http://www.chem.ox.ac.uk/icl/heyes/structure_of_solids/lecture1/lec1.html>

[21] J-G. Hyun, S. Lee, S-D. Cho, K-W. Paik. *Frequency and Temperature Dependence of Dielectric Constant of Epoxy/$BaTiO_3$ Composite Embedded Capacitor Films (ECFs) for Organic Substrate.* Electronic Components and Technology Conference. (2005)

[22] A. J. Bosman, E. E. Havinga. *Physical Review Letters.* **129**, 4 (1963)

[23] R. Kotz, M. Carlen. *Electrochimica Acta.* **45,** 2483-2498 (2000)